Anatomical Science International
https://doi.org/10.1007/s12565-026-00974-2

REVIEW

The anterior condylar confluence of Trolard and its venous tributaries: an anatomical review

Mugurel Constantin Rusu[1] · **Adelina Maria Jianu**[2,3] · **Petrinel Mugurel Rădoi**[4] · **Răzvan Costin Tudose**[1]

Received: 12 August 2026 / Accepted: 15 September 2026
© The Author(s) 2026

Abstract

The anterior condylar confluence (ACC) of Trolard is a small extracranial venous plexus at the external orifice of the hypoglossal canal. Described over 150 years ago and present in the classical French anatomical literature, it was largely absent from the Anglophone radiological and surgical literature until the corrosion-cast study of San Millán Ruíz et al. (2002). It is the venous crossroads of the craniocervical junction, linking the posterior fossa dural sinuses, the internal jugular vein and the vertebral venous system. This structured anatomical review, illustrated with retrospectively selected MR and CT angiographic examinations, synthesises the anatomy of the confluence and of the ten venous channels reported to communicate directly or indirectly with ACC territory: the anterior, lateral and posterior condylar veins, branches of the internal jugular vein and its bulb, the inferior petrosal sinus, the inferior petro-occipital vein, the internal carotid artery venous plexus of Rektorzik, the prevertebral venous plexus, the marginal sinus and the clival diploic veins. For each, we collate the reported prevalence, osseous conduit, connected territories, and clinical relevance, and we state the denominators explicitly, since they differ by cast, side, junction, and subject. Two themes recur. The confluence is valveless throughout and reverses its drainage direction with posture, so the channels that join it form a bidirectional network rather than tributaries of a sinus. Targeted anatomical and imaging studies consistently identified the ACC, whereas the visibility and reported prevalence of several individual connections varied substantially across methods. Knowledge of this anatomy is required for far-lateral, transcondylar and endoscopic approaches, for transvenous access to the cavernous sinus, and for recognising fistulae of the region.

Keywords Anterior condylar confluence · Hypoglossal canal · Condylar veins · Venous plexus of Rektorzik · Craniocervical venous system

Abbreviations

ACC	Anterior condylar confluence (confluent)
ACV	Anterior condylar vein
AEVVP	Anterior external vertebral venous plexus
AIVVP	Anterior internal vertebral venous plexus
CDV	Clival diploic vein
CS	Cavernous sinus
CT	Computed tomography
CT-DSV	Computed tomography digital subtraction venography
CTA	Computed tomography angiography
DAVF	Dural arteriovenous fistula
HC	Hypoglossal canal
ICA	Internal carotid artery
IJV	Internal jugular vein
IPOV	Inferior petro-occipital vein
IPS	Inferior petrosal sinus

✉ Răzvan Costin Tudose
razvan-costin.tudose0721@stud.umfcd.ro

[1] Division of Anatomy, Faculty of Dentistry, "Carol Davila" University of Medicine and Pharmacy, 020021 Bucharest, Romania

[2] Department of Anatomy and Embryology, Faculty of Medicine, "Victor Babeş" University of Medicine and Pharmacy, 300041 Timişoara, Romania

[3] Municipal Emergency Clinical Hospital of Timişoara, 300041 Timişoara, Romania

[4] Division of Neurosurgery, Department 6, Clinical Neurosciences, Faculty of Medicine, "Carol Davila" University of Medicine and Pharmacy, 020021 Bucharest, Romania

Published online: 19 September 2026

JB	Jugular bulb
JTVC	Jugular tubercle venous complex
LCV	Lateral condylar vein
MRI	Magnetic resonance imaging
MS	Marginal sinus
MSCT	Multi-slice computed tomography
PCC	Posterior condylar canal
PCEV	Posterior condylar emissary vein
PCV	Posterior condylar vein
SCS	Suboccipital cavernous sinus
SS	Sigmoid sinus
VAVP	Vertebral artery venous plexus
VPR	Venous plexus of Rektorzik
VVP	Vertebral venous plexus

Introduction

The venous anatomy of the craniocervical junction is among the most complex and clinically relevant vascular territories of the human body. It provides the connections between the intracranial dural venous sinuses and the extracranial cervical venous systems. It is critically involved in the physiological redirection of cerebral venous blood with postural change (San Millán Ruíz et al. 2002; Kosugi et al. 2020). Despite this importance, several structures of the craniocervical venous system were historically overlooked.

The anterior condylar confluence (ACC), first described by Jean Baptiste Paulin Trolard in his 1868 doctoral thesis at the Faculty of Medicine of Paris (Trolard 1868; Loukas et al. 2010), is one such structure. Trolard described a venous plexiform structure located extracranially, anterior to the hypoglossal canal opening, which received multiple tributaries and served as a nodal point for venous redistribution at the skull base. Despite this early description, the ACC was virtually ignored in the radiologic and surgical literature for over 130 years.

The modern rediscovery of the ACC stemmed from the landmark corrosion cast study by an Millán Ruíz et al. (2002), which systematically demonstrated the ACC's near-constant presence, its six main tributaries, and its connections to the posterior fossa dural sinuses, the internal jugular vein (IJV), and the vertebral venous systems. Since then, the ACC has been recognised as a major venous crossroad, also termed the 'petrosal confluence' by Katsuta et al. (1997). The structure has also been implicated in the pathophysiology of dural arteriovenous fistulae (DAVFs) of the HC, which account for 1.8–4.2% of all intracranial DAVFs in single-centre series (Choi et al. 2013; Spittau et al. 2015; Iampreechakul et al. 2025).

This review aims to provide a comprehensive anatomical synthesis of the ACC and its venous tributaries, drawing upon evidence retrieved from major bibliographic databases. Each tributary is discussed in a dedicated subsection, addressing its morphology, variability, prevalence, and clinical relevance. This structured anatomical review draws on the published literature; original MR and CT angiographic examinations from anonymised institutional archives illustrate the described anatomy and are not analysed as a cohort. Where an illustrated configuration is compared with earlier descriptions, the comparison is descriptive and carries no prevalence claim.

Materials and methods

Literature search and source selection

We searched PubMed, Scopus, and Web of Science Core Collection from inception to 30 July 2026. Three strands were run separately in each database: Strand 1 for broad anterior condylar confluence and anterior condylar vein anatomy, Strand 2 for inferior petrosal sinus termination and drainage, and Strand 3 for fistulae of the confluence and HC and their endovascular treatment. Each strand combined two or three predefined concept blocks. Searches were restricted to Title/Abstract fields in PubMed, TITLE-ABS-KEY fields in Scopus, and Topic (TS) fields in Web of Science Core Collection, without language or date restriction; the verbatim strings are reproduced in Supplementary Material 1. The nine exports returned 675 records, and de-duplication on DOI, then PMID, then normalised title removed 391 duplicate occurrences, leaving 284 de-duplicated records. The 284 de-duplicated records were triaged on title and abstract into five categories: core anatomy and imaging of the confluence and the anterior condylar vein (22 records); reports of fistulae of the confluence or HC and their endovascular treatment (95); directly associated venous anatomy of the inferior petrosal sinus, the plexus of Rektorzik, the petro-occipital and prevertebral pathways, the suboccipital cavernous sinus (SCS), the marginal sinus and the condylar routes (99); false positives retrieved by the term Trolard but concerning the superior anastomotic cortical vein (7); and records outside the scope of the confluence and the inferior petrosal sinus (61). This review draws on the 121 records in the two anatomical categories—core anatomy and imaging of the confluence, and directly associated venous anatomy—together with the classical and mid-twentieth-century sources cited within them, which predate database coverage and were retrieved by hand. We cite reports of fistulae here only when they document venous anatomy, and we treat them systematically in a companion review.

We triaged and selected records as follows. A record entered one of the two anatomical categories when its title

or abstract reported, in human subjects or specimens, the morphology, prevalence, dimensions, connections or imaging appearance of the confluence, of the anterior condylar vein, or of one of the associated channels named above (the inferior petrosal sinus and its caudal termination, the inferior petro-occipital vein, the plexus of Rektorzik, the prevertebral and precondylar veins, the SCS, the marginal sinus, the condylar canals and veins, and the clival venous channels). Records were excluded after title and abstract triage when they concerned the superior anastomotic vein of Trolard; reported a fistula, tumour or other lesion without describing normal or variant venous anatomy; dealt with the intracranial inferior petrosal sinus or the cavernous sinus without reference to the caudal termination; or were non-human, editorial or duplicate publications. We applied no restrictions based on study design, sample size, imaging modality, or year. Triage was performed by one author and checked by a second; the full texts of all 121 records in the two anatomical categories were read by both, and disagreements were resolved by consensus. We identified classical and mid-twentieth-century sources that predate database coverage through reference lists and historical accounts of the retrieved records, and consulted them in their original form.

Only 89 of the 284 de-duplicated records were returned by all three databases (109 were unique to Scopus, 28 to Web of Science, and 26 to PubMed), so a search confined to any single database would have missed much of this literature.

We conducted the search systematically and report it in full. Still, this article is a structured anatomical review rather than a systematic review in the PRISMA sense: beyond the relevance rules stated above, no formal study-level eligibility criteria were applied, title and abstract triage was not performed independently in duplicate, no risk-of-bias or study-quality assessment was made, and no study-level inclusion flow is reported. A PRISMA flow diagram is not provided because the unit of this review is the anatomical structure rather than the study, and the records contribute descriptive data rather than pooled estimates; the record-level flow (675 records retrieved, 284 after de-duplication, 121 in the two anatomical categories) is given above, and the counts for each of the nine searches are listed in Supplementary Material 1.

Illustrative angiographic material and image analysis

Original anonymised craniocervical MR angiographic and CT angiographic examinations, previously acquired for clinical indications unrelated to this review, were retrospectively selected to illustrate the ACC and its associated venous channels. The images constituted a pictorial anatomical dataset and were not analysed as a consecutive prevalence cohort. The examinations were fully anonymised before retrieval, so age, sex, and clinical indication were unavailable and are not reported. We selected examinations that were technically adequate, in which the venous channels of the craniocervical junction were opacified and could be followed on the source images; selection was therefore purposive, not consecutive, and the material cannot be used to estimate the frequency of any configuration.

MR angiography had been performed on a 1.5-T MAGNETOM Amira (Siemens Healthineers) scanner using a time-of-flight (TOF) three-dimensional sequence. Acquisition parameters were: repetition time, 25 ms; echo time, 7 ms; flip angle, 20°; field of view, 200 × 181 mm; acquisition matrix, 320 × 224; section thickness, 0.7 mm; and reconstructed voxel size, 0.6 × 0.8 × 0.7 mm. The MR examinations were performed without contrast material. CT angiography was performed on a 32-slice scanner (Siemens Perspective, Siemens Healthineers, Forchheim, Germany) with 0.6 mm collimation and 0.75 mm reconstructed slice thickness with 50% overlap, as in previous reports from this group (Tudose et al. 2026), and the CT data were analysed with Horos 3.3.6 (Horos Project, Annapolis, MD, USA). The illustrative dataset comprised 20 MR angiographic examinations and 20 CT angiographic examinations from 40 subjects.

Source images were reviewed in the axial, coronal and sagittal planes. Multiplanar and curved-planar reformations, maximum-intensity projections and three-dimensional volume-rendered reconstructions were used to trace the confluence, condylar veins, inferior petrosal sinus, inferior petro-occipital vein, venous plexus of Rektorzik, jugular bulb and internal jugular vein, marginal sinus, prevertebral plexus and vertebral venous channels. We accepted a vessel as a distinct venous channel only when we could follow its continuity on sequential source images or multiplanar reformations; we used three-dimensional renderings for spatial orientation and illustration. In selected reconstructions, we digitally suppressed overlying venous structures without altering the source data. We assessed CT angiographic material from thin-section source images, multiplanar reformations, and three-dimensional volume rendering. Two authors reviewed all examinations jointly, and they accepted each labelled structure by consensus. We did not tally the presence or absence of any channel per subject, because the dataset was assembled for illustration, not measurement.

Ethical considerations

The literature-review component did not involve human participants. The angiographic material was retrospectively

selected from anonymised examinations acquired for clinical purposes; no additional imaging or intervention was performed, and all identifiers were removed before analysis and figure preparation. The research was conducted ethically in accordance with the Declaration of Helsinki. The study was approved by the Ethics Committee of the Municipal Emergency Clinical Hospital of Timișoara (approval no. E−4247/15.10.2025).

Terminology and conventions

Three conventions are used throughout. First, 'tributary' is used in its morphological sense, for a channel that joins the confluence, and implies no fixed direction of flow: every channel described here is valveless, and its flow reverses with posture (Section "Postural Venous Haemodynamics"). Where the physiological relationship is at issue, 'connection' or 'communicating channel' is used instead. Second, anatomical constancy, which only dissection or corrosion casting can establish, is distinguished from consistent visualisation within an imaging series, which depends on modality, acquisition technique, flow direction and the position of the subject; a channel not opacified on a supine acquisition is not thereby shown to be absent. Third, the vein beneath the petro-occipital fissure is called the inferior petro-occipital vein rather than the inferior petroclival vein. Neither term appears in Terminologia Anatomica, so the preference is topographic and historical rather than nomenclatural: the vein follows the petro-occipital fissure and lies remote from the clivus proper, and 'petro-occipital' is the term of Trolard (1868) and of the classical French literature; 'inferior petroclival vein' is retained where the cited authors used it. The venous compartment around the third segment of the vertebral artery is called the suboccipital cavernous sinus, after Arnautovic et al. (1997); the alternative 'suboccipital venous plexus' is given once (Section "Surgical and Endovascular Implications") so that both terms can be searched.

General anatomy of the ACC

The ACC is an extracranial venous structure located in the anterior condylar fossa, directly anterior to the external orifice of the HC (San Millán Ruíz et al. 2002; Tudose et al. 2024). It lies medial to the IJV and antero-inferior to the JB, just below the termination of the inferior petrosal sinus (Spittau et al. 2015). In the corrosion cast study by San Millán Ruíz et al. (2002), the ACC measured 3–5 mm in an anterior (frontal) view and approximately 2 mm in its ventrodorsal extent. Spittau et al. (2015) described the ACC as a consistently observed small venous structure with a maximal diameter of approximately 5 mm (Takemoto et al. 2014; Spittau et al. 2015). Takahashi et al. (2005) identified the ACC bilaterally in all 33 patients examined with contrast-enhanced 3D MR imaging of the craniocervical junction, and described it as a central venous confluence connecting the JB, anterior condylar vein, inferior petro-occipital vein (IPOV; also referred to as inferior petroclival vein), and inferior petrosal sinus.

Structurally, the ACC functions as a venous plexus or confluence rather than a discrete sinus. The venous anatomy at the JB, including its connections with the condylar emissary veins and the plexus of Rektorzik, was comprehensively documented in the French anatomical tradition by Paturet (1958), who listed among the afferents of the JB ('golfe de la jugulaire') the inferior petrosal sinus, the sinus pétro-occipital d'Englisch, the anterior condylar emissary veins, and branches from the sinus carotidien de Rektorzik (Paturet 1958). San Millán Ruíz et al. (2002) identified six veins regularly contributing to the formation of the ACC, listed in Table 2 and mapped in Fig. 1 (San Millán Ruíz et al. 2002). Figure 1 provides a box–circle–connector reinterpretation of San Millán Ruíz et al.'s Fig. 8 and should be understood as a synoptic map of relationships rather than as a morphological classification. Importantly, although the Rektorzik pathway is recognised in the text of San Millán Ruíz et al., their Fig. 8 does not explicitly depict the inferior petro-occipital vein as a distinct labelled channel.

In the reviewed material, the relevant descriptions remain those of a petrosal venous confluence, a plexiform caudal IPS termination, suboccipital CS/condylar venous connections, and a prevertebral/precondylar midline "necklace"; none of these studies presents the distal IPS–IJV pathway or the ACC as a named ring-shaped structure (Katsuta et al. 1997; Takahashi et al. 2005; Mitsuhashi et al. 2007; Matsushima et al. 2015; Matsuo et al. 2021; Yamada et al. 2022). The closest anatomical construct is the petrosal venous confluence: the caudal IPS, immediately before or at the jugular foramen, may form a confluence with the ACV, IPOV and LCV (Matsuo et al. 2021). This construct should be distinguished from the prevertebral/precondylar "necklace" appearance (Fig. 2), which represents midline fusion of ventral craniocervical veins and not an annular ACC or a specific IPS–IJV ring (Yamada et al. 2022). Figure 3 illustrates a ring-shaped IPS–IJV configuration. The term 'IPS–IJV ring' is used here as a descriptive morphological label for that appearance and not as a newly defined anatomical entity. The configuration itself has been depicted before. Zhang et al. (2010a), reclassifying the caudal termination of the IPS on multislice CT in 120 patients (239 sides), describe two subtypes in which the extracranial IPS reaches the internal jugular vein through two separate junctions, one low and one high: their pattern C-2 (31 sides, 12.9%) and pattern C-3 (15 sides, 6.3%), the latter additionally communicating with the sigmoid sinus

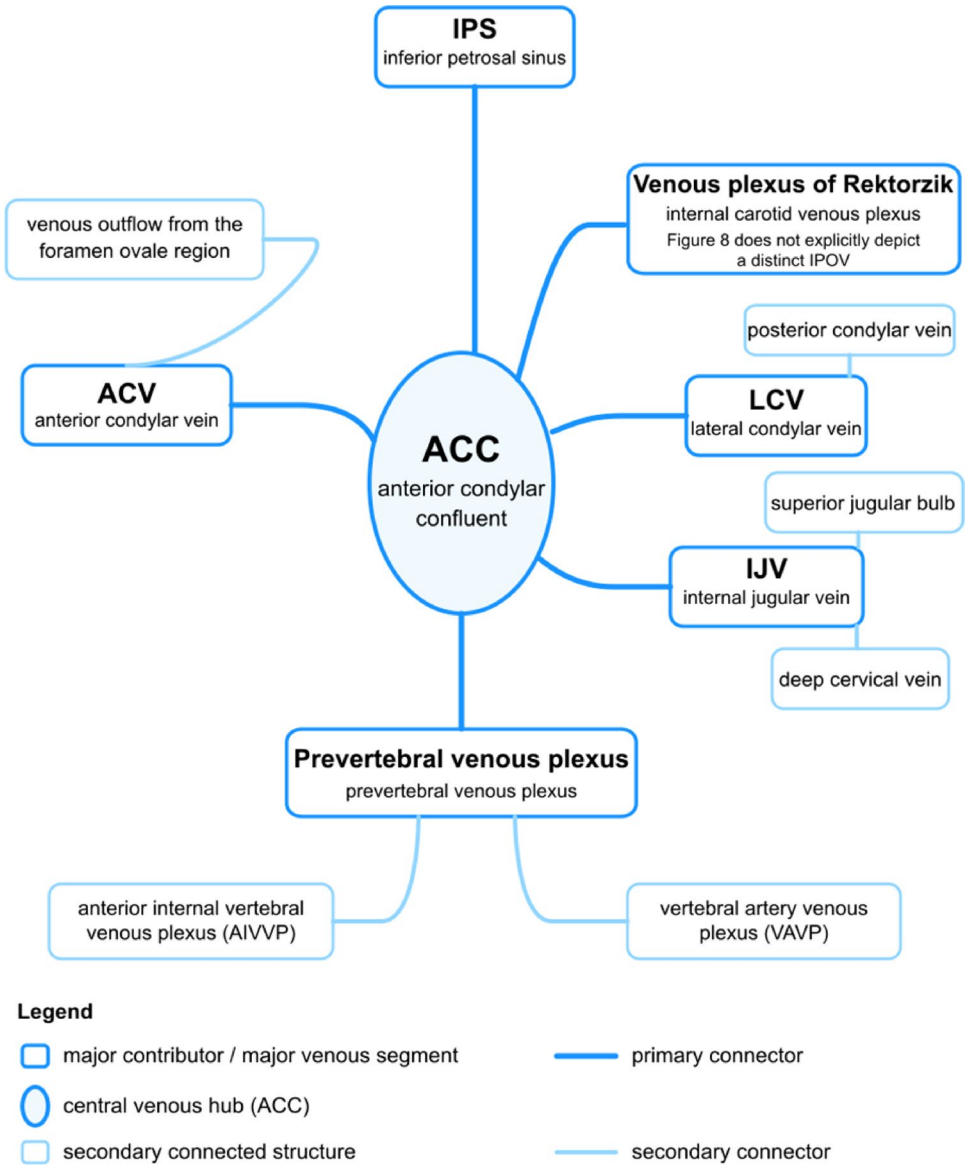


Fig. 1 Box–circle–connector reinterpretation of San Millán Ruíz et al. Fig. 8. Schematic reinterpretation of the anterior condylar confluence (ACC) and its principal venous connections, based on the schematic anterior view published by San Millán Ruíz et al. (2002). The central circle represents the ACC at the external orifice of the hypoglossal canal. Rounded boxes indicate the six principal contributors named in the original caption; secondary boxes show adjacent continuities represented or implied in the original scheme. Connectors indicate anatomical relationships, not flow direction. The figure is a synoptic reinterpretation of published relationships and not a morphological classification

(Zhang et al. 2010a). Together, these account for 46 of 239 sides (19.2%). Because the two limbs of the sinus and the intervening segment of the internal jugular vein enclose a space, the configuration illustrated in their Fig. 3c and e is annular. It corresponds to the appearance illustrated in Fig. 3. Zhang et al. (2010a) nevertheless treat these subtypes as a matter of the number of confluence points rather than of shape: the ring is depicted but is neither named nor analysed as a closed structure, and no relationship to the ACC is drawn (Zhang et al. 2010a). The present material therefore adds only an explicit descriptive label and an MR angiographic illustration of a configuration already depicted by Zhang et al. (2010a). Because the illustrative examinations were selected rather than consecutive, no frequency for the configuration can be derived from them, and the only available estimate remains 46 of 239 sides (19.2%) from that multislice CT series, obtained with a different definition and unit of analysis. Figure 4 shows the direct anastomosis between the IPS and the IPOV that contributes to the petrosal venous confluence and is discussed in Section "The Inferior Petro-Occipital Vein".

Less constant connections include the posterior condylar vein, the MS, and clival diploic veins (Tanoue et al. 2005; Mizutani et al. 2017; Tudose et al. 2024).

The ACC contains valveless veins, allowing multidirectional venous flow (San Millán Ruíz et al. 2002; Spittau et al. 2015). This characteristic is functionally critical, as it permits the confluence to reverse its drainage direction with posture; quantitative evidence is presented in Section "Postural Venous Haemodynamics". Figure 5 shows the confluence and tributaries described here in angiographic material.

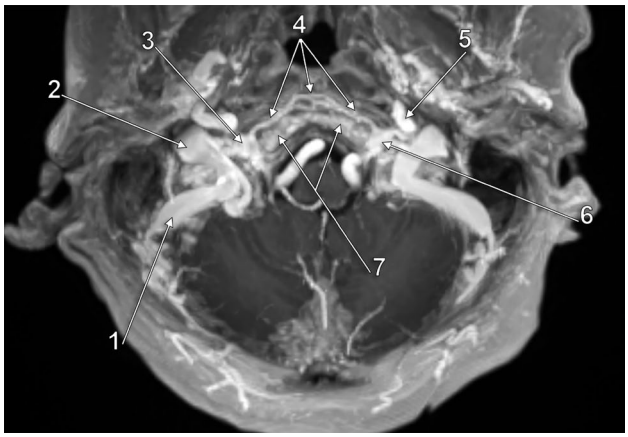


Fig. 2 The prevertebral vein or plexus at the level of the atlas. MR angiogram. Axial slice through the anterior arch of the atlas. 1. right sigmoid sinus; 2. right internal jugular vein; 3. right anterior condylar confluence; 4. the prevertebral vein-plexus-vein morphology; 5. left internal carotid artery; 6. left anterior condylar confluence; 7. anterior arch of the atlas. The plexiform middle segment lies between two single-channel ends, and both confluences are connected to it

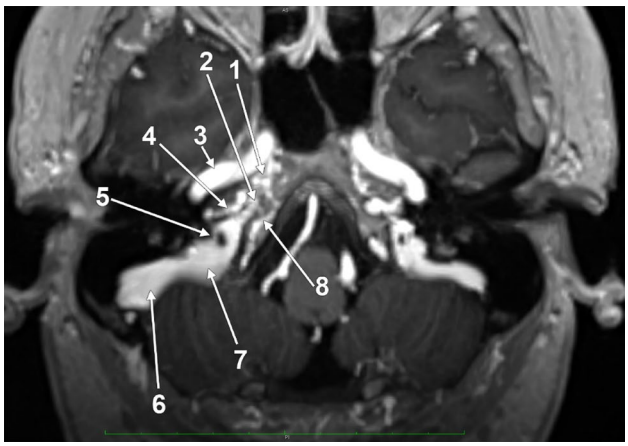


Fig. 3 A ring-shaped configuration at the junction of the inferior petrosal sinus (IPS) and the internal jugular vein (IJV). MR angiogram. Curved-planar axial slice. 1. plexus of Rektorzik; 2. IPS; 3. internal carotid artery; 4. transpetrous communicating vein; 5. ring-shaped IPS–IJV configuration ('IPS–IJV ring', a descriptive term; see text); 6. sigmoid sinus; 7. jugular bulb; 8. inferior petro-occipital vein

Table 1 summarises cross-study prevalence and visibility data for the ACC and its tributaries.

ACC anterior condylar confluence, *ACV* anterior condylar vein, *LCV* lateral condylar vein, *PCV* posterior condylar vein, *IPS* inferior petrosal sinus, *IPOV* inferior petro-occipital vein, *VPR* venous plexus of Rektorzik, *Prevert.* prevertebral, *CDV* clival diploic vein, *bilat* bilateral, *unilat* unilateral, *asym* asymmetry, *agen* agenesis, *conn.* connection, *R* right, *L* left, *JB* jugular bulb type, *SS* sigmoid sinus type, *ACEV* anterior condylar emissary vein type, *OS* occipital sinus type, *CT-DSV* computed tomography digital

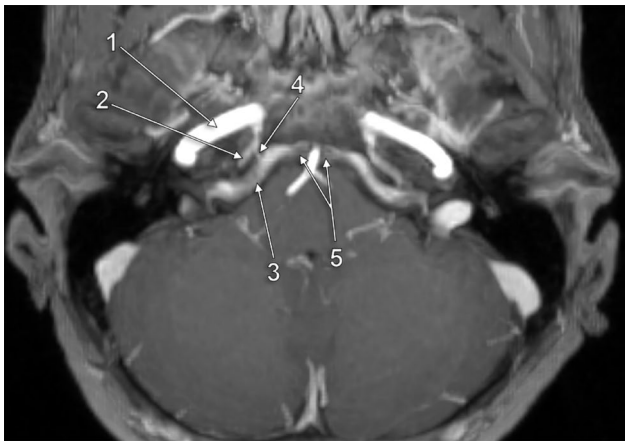


Fig. 4 The anastomosis of the inferior petrosal sinus with the inferior petro-occipital vein. MR angiogram. Curved-planar axial slice. 1. inferior petro-occipital vein; 2. internal carotid artery; 3. inferior petrosal sinus; 4. anastomosis of the inferior petrosal sinus with the inferior petro-occipital vein; 5. basilar venous plexus

subtraction venography, *CTA* computed tomography angiography, *surg* surgical, *pts* patients, *dep.* dependent, *quantif.* quantified

*CDV prevalence 14% per Mizutani et al. (2017), not assessed in the above studies. Additional PCC bony canal data: Matsushima 2014: 82% (CT); Lucena 2025: bilat 46.6–54%, absent 10–23.1%.

Venous tributaries of the ACC

The principal venous tributaries of the ACC and their clinical relevance are synthesised in Table 2.

The anterior condylar vein

The anterior condylar vein (ACV) is the most functionally significant tributary of the ACC. Designated the 'venous plexus of the hypoglossal nerve' in the international anatomic nomenclature (San Millán Ruíz et al. 2002), it traverses the HC alongside the hypoglossal nerve and branches of the ascending pharyngeal artery, providing a critical link between the ACC and the anterior internal vertebral venous plexus (AIVVP) (San Millán Ruíz et al. 2002; Natsis and Piagkou 2015; Spittau et al. 2015).

In the corrosion cast study, the ACV was present on all but one side (96% of sides), appearing as a plexiform connection between the AIVVP and the ACC (San Millán Ruíz et al. 2002). In six of 24 sides (25%), small plexiform anastomoses were observed with the basilar plexus. On occasion, the ACV was traversed longitudinally by a channel for the hypoglossal nerve. Tanoue et al. (2010) found that in all 50 CT-examined cases, the ACVs connected the ACC to

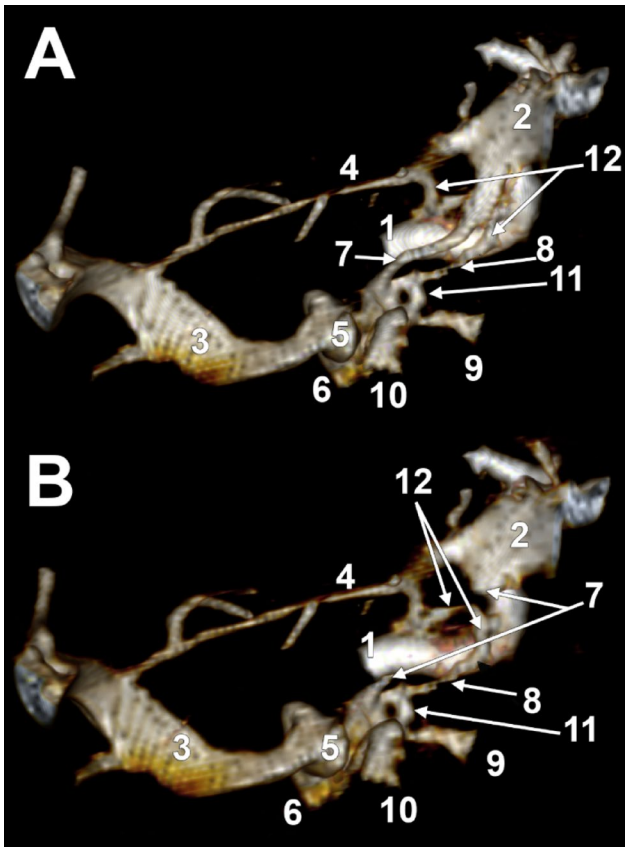


Fig. 5 The venous anatomy anterior to the initial segment of the internal jugular vein. MR angiogram. Three-dimensional volume rendering. Left side, medial view. **A** complete inferior petrosal sinus; **B** inferior petrosal sinus digitally removed to expose the confluence. 1. internal carotid artery; 2. cavernous sinus; 3. sigmoid sinus; 4. superior petrosal sinus; 5. jugular bulb; 6. internal jugular vein; 7. inferior petrosal sinus; 8. inferior petro-occipital vein of Trolard; 9. anterior condylar vein; 10. posterior condylar vein; 11. anterior condylar confluence; 12. venous plexus of the internal carotid artery (plexus of Rektorzik). The edited view in B shows the confluence receiving the anterior and posterior condylar veins, the inferior petro-occipital vein and the plexus of Rektorzik at a single point

the MS. The ACV is the cranial extension of the AIVVP. It may connect intracranially and extradurally with the basilar plexus (Tubbs et al. 2007), which in turn allows indirect connections with the posterior compartment of the CS and with the anterior pial brainstem veins via emissary bridging veins (Spittau et al. 2015). As one of the cranial emissary veins, the ACV participates in the extracranial drainage of the posterior fossa dural sinuses (Okudera et al. 1994; Mortazavi et al. 2012).

Mizutani et al. (2018) identified a previously unnamed intraosseous venous structure within the jugular tubercle, superomedial to the HC, which they designated the jugular tubercle venous complex (JTVC). Using CT-DSV in 50 normal controls, the JTVC was visualised in 46.0% of sides and was always continuous with the ACV (Mizutani et al. 2018a). In a series of seven patients with ACC-DAVFs examined by cone-beam CT, fistulous pouches lay in the JTVC, the ACV proper, or other exoccipital channels in roughly equal proportions, and the ACV–JTVC channel was involved in two-thirds of cases (Mizutani et al. 2018a). The JTVC is therefore a normal variant with a preferential role in ACC-DAVFs formation, and cone-beam CT delineates it during embolisation.

The same study mapped the broader intraosseous network of the JTVC: osseous connections were reported, in decreasing order of frequency, with the PCV, the jugular vein or bulb, the inferior petroclival vein, the LCV, the MS, the CDV, the ACC and the IPS (39.1% to 6.5% of the 46 JTVC sides) (Mizutani et al. 2018a). The JTVC is therefore better regarded as a multidirectional intraosseous extension of ACV territory than as a single additional tributary.

The lateral condylar vein

The lateral condylar vein (LCV) was observed in 79% of sides (19 of 24) in the corrosion cast study (San Millán Ruíz et al. 2002). Its origin was generally found on an anastomotic branch between the ACC and the IJV, and not directly on the IJV as described by Arnautovic et al. (1997).The LCV is connected with the vertebral artery venous plexus in the atlanto-occipital space.

Matsushima et al. (2015) provided the most detailed morphological study of the LCV, identifying it in 88.0% of paracondylar areas with an average diameter of 3.6 mm. The LCV was classified into two types based on its origin: type 1, originating from the ACC; and type 2, originating from the IJV. In some specimens, the LCV coursed within a small osseous canal lateral to the occipital condyle–the paracondylar canal–identified in 16.7% of dry bone specimens. Using contrast-enhanced 3D MR imaging, Takahashi et al. (2005) identified the LCV (Table 1) connecting the external orifice of the ACV and the anterolateral portion of the suboccipital CS. The LCV is related to the external vertebral venous system and may become a major drainage pathway in cases of ACC-DAVFs (Spittau et al. 2015).

Understanding LCV anatomy is important for far-lateral transcondylar surgical approaches, where it may be encountered during exposure of the JB, HC, or foramen magnum (Matsushima et al. 2015).

Branches from the internal jugular vein and its bulb

The ACC is connected to the IJV and its superior bulb through one or several bridging veins (San Millán Ruíz et al. 2002; Tudose et al. 2024). These connections allow for bidirectional flow between the ACC and the jugular system. In the corrosion cast study, branches from the IJV or its bulb

Table 1 Synoptic prevalence of the ACC and its tributaries across imaging and cadaveric studies

Structure	San Millán Ruíz et al. (2002) (casts, 24 sides)	Tanoue et al. (2010) (CT, 50 pts)	Caruso et al. (1999) (MRI, 14 pts)	Takahashi et al. (2005) (MRI, 33 pts)	Pekçevik and Pekçevik (2014) (CTA, 166 pts)	Imai et al. (2022) (CT-DSV, 253 pts)	Yamada et al. (2022) (CT-DSV, 273 pts)	Ota et al. (2017) (surg, 104 sides)
ACC	100%	100%	–	100% bilat (33/33)	–	–	–	–
ACV	96% (23/24)	100%	–	100% bilat (33/33)	–	–	–	–
LCV	79% (19/24)	Asym/agen noted	–	54.5% bilat 18.1% unilat	–	–	–	–
PCV	79% (19/24)	Asym/agen noted	33–67% (plane-dep.)	63.6% bilat 30.3% unilat	58.4% bilat 18.1% unilat absent 23.5%	–	–	83.7% JB 40.3% SS 31.7% ACEV 7.7% OS 1.0% absent 16.3%
IPS→ACC	Constant	Variable	–	–	–	–	–	–
IPOV	Constant	–	–	–	–	–	–	–
VPR	present (not quantif.)	–	–	–	–	24% (60/253) (71/506 sides, 14%) R>L p=0.0002 ACC conn. 38% (27/71)	–	–
Prevert vein	constant	–	–	–	–	–	54% (297/546 sides) (R 154/273, L 143/273) ACC conn. 95% fusion 42% (115/273)	–
Marginal sinus	83.3% (10/12 casts)	–	–	–	–	–	–	–
CDV	–*	–	–	–	–	–	–	–

Reported frequencies are descriptive and should not be compared directly across studies, because populations, methods, anatomical definitions and units of analysis (casts, sides, patients) differ; numerators and denominators are given where the source reports them

were one of the six regular contributors (San Millán Ruíz et al. 2002).

These bridging veins permit retrograde venous flow into the sigmoid and transverse sinuses in cases of DAVF (Spittau et al. 2015). Tudose et al. (2024) provided MR angiographic 3D volume renderings demonstrating these bridging veins connecting the ACC to the JB. In cases of IJV compression or thrombosis, the ACC and its collateral pathways become functionally critical for cerebral venous drainage. A recently described clinically relevant mechanism is styloid process–mediated compression of the IJV at the level of the transverse process of the atlas (Eagle jugular syndrome), which may generate venous hypertension sufficient to promote DAVF formation at the ACC (Suzuki et al. 2020; Rusu et al. 2025b).

The inferior petrosal sinus

The inferior petrosal sinus (IPS) is a major dural venous sinus that courses along the petroclival fissure from the CS to the jugular foramen region. Its caudal termination shows considerable variability and directly involves the ACC (San Millán Ruíz et al. 2002; Mitsuhashi et al. 2007; Zhang et al. 2010a; Mizutani 2024).

IPS-IJV junction classification. The classical classification by Shiu et al. (1968), later refined by Miller et al. (1993), identified four types of IPS drainage (Shiu et al. 1968; Miller et al. 1993; Zhang et al. 2010a). Rubinstein et al. (1995), in a detailed CT and cadaveric study of 39 jugular foramina, found the IPS joining the jugular venous system within the foramen, at its exocranial opening or below the skull base in 4, 8 and 15 cases, respectively (Rubinstein et al. 1995). The long extracranial extension of the IPS, first characterised systematically by Gailloud et al. (1997), is treated in Section "The Long Inferior Petrosal Sinus" (Gailloud et al. 1997).

Using 3D rotational venography of 83 sides, Mitsuhashi et al. (2007) classified the caudal termination of the IPS into six types (A–F), with type C subdivided into C-1 and C-2, yielding the seven drainage patterns depicted in Fig. 6

Table 2 Synthesis of the venous tributaries of the anterior condylar confluence

Tributary	Other designations	Osseous conduit/landmark	Territories connected	Reported prevalence (source)	Principal clinical relevance
Anterior condylar vein (ACV)	Venous plexus of the hypoglossal nerve (Terminologia Anatomica)	Hypoglossal (anterior condylar) canal	AIVVP ↔ ACC	96% of sides (23/24) San Millán Ruíz 2002; 100% Takahashi 2005 (San Millán Ruíz et al. 2002; Takahashi et al. 2005)	principal route to the VVP; dense coil packing within the canal risks hypoglossal nerve palsy
Lateral condylar vein (LCV)	–	paracondylar canal when present (16.7% of areas, Matsushima 2015)	ACC / IJV ↔ VAVP at C1–C2	79% of sides (19/24) San Millán Ruíz 2002; 88.0% of paracondylar areas Matsushima 2015 (San Millán Ruíz et al. 2002; Matsushima et al. 2015)	LCV was identified as a drainage channel in 7 of 8 ACC-DAVFs (Miyachi et al. 2008)
Branches from the IJV or its bulb	Bridging veins	jugular foramen region	ACC ↔ IJV / jugular bulb	constant in casts (San Millán Ruíz et al. 2002)	the standard transjugular access corridor to the ACC
Inferior petrosal sinus (IPS)	–	anterior compartment of the jugular foramen	cavernous sinus ↔ ACC / IJV	anastomosis with the ACC in every specimen (San Millán Ruíz et al. 2002); termination types in Table 3	retrograde corridor to CS and superior ophthalmic vein; explains ocular presentation of ACC-DAVFs
Inferior petro-occipital vein (IPOV)	Inferior petroclival vein; sinus pétro-occipital d'Englisch	petro-occipital (petroclival) fissure	VPR ↔ superior jugular bulb / ACC	83.3% of sides (20/24) (Tubbs et al. 2014); communicates with hypoglossal-canal veins in 20%	alternative transvenous access to the CS (Kurata et al. 2012); radiologically confusable with the IPS
ICA venous plexus of Rektorzik (VPR)	Sinus carotidien de Rektorzik	carotid canal	cavernous sinus ↔ ACC	24% of patients (60/253), 14% of sides (71/506) on CT-DSV (Imai et al. 2022); proximal connection to the ACC 27/71 (38%)	encountered in endonasal exposure of the petrous ICA; ACC–CS shunt corridor
Prevertebral venous plexus	Prevertebral vein; precondylar vein (Yamada et al. 2022)	anterior atlanto-occipital membrane; basiocciput	ACC ↔ midline, contralateral ACC, AEVVP	vein present on 56% right (154/273) / 52% left (143/273), of which 95% connect to the ACC (Yamada et al. 2022); midline fusion 42%	cross-midline corridor for contralateral transvenous access
Posterior condylar vein (PCV)	Condylar emissary vein (Terminologia Anatomica)	posterior condylar canal	sigmoid sinus / JB ↔ suboccipital plexus, deep cervical vein, VAVP	79% of sides (19/24) San Millán Ruíz 2002; 83.7% Ota 2017 (JB origin 40.3%) (San Millán Ruíz et al. 2002; Ota et al. 2017)	distinct posterior condylar canal DAVF entity; landmark in the far-lateral approach
Marginal sinus (MS)	–	dural margin of the foramen magnum	ACV ↔ occipital sinus, suboccipital veins	83.3% of cases (10/12) San Millán Ruíz 2002; connected anteriorly to the ACV in all	fistulas historically labelled "marginal sinus DAVF" are frequently ACC/HC lesions
Clival diploic vein (CDV)	Transclival emissary vein	clivus	basilar plexus / VPR ↔ ACC region	14.0% (Mizutani et al. 2017)	occasional distal connection of the VPR (Imai et al. 2022)

Reported frequencies are descriptive and should not be compared directly across rows because populations, methods, anatomical definitions and units of analysis differ; numerators and denominators are given where the source reports them

San Millán Ruíz et al. (2002) listed six regular contributors: the ACV, branches from the IJV or its bulb, the LCV, anastomoses with the IPS, branches from the ICA venous plexus of Rektorzik via the IPOV, and branches from the prevertebral venous plexus. The PCV, the MS and the clival diploic veins are additional connections documented subsequently and are not part of that original list. Percentages are per side unless otherwise stated. It should be noted that the six contributors constitute an inventory of tributaries and not a morphological classification: they are nowhere combined into types or grades, and no frequency is attached to any pattern of the confluence itself, only to its individual tributaries

and listed in Table 3 (Mitsuhashi et al. 2007). Zhang et al. (2010a), using MSCT on 120 patients (239 sides), found the IPS draining into the VVP via the ACV in 218 sides and via the LCV in 100 sides. The venous diameter at the IPS-IJV confluence ranged from 0.8 to 5.7 mm (mean 2.51 mm) and was significantly larger on the right side ($p = 0.01$).

The IPS is the main transvenous access route for endovascular treatment of CS and ACC lesions (Mitsuhashi et al. 2007; Spittau et al. 2015) and knowledge of its caudal anatomy is critical for catheter navigation.

Table 3 summarises the main classification systems and variants of the IPS caudal termination.

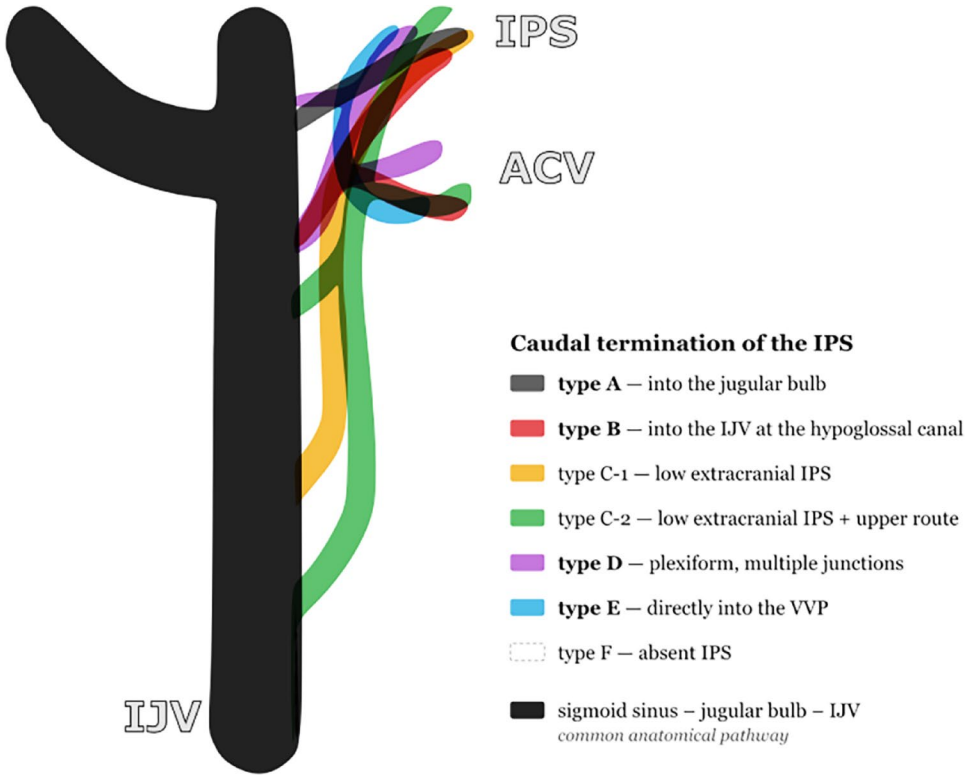


Fig. 6 Mitsuhashi classification of the caudal termination of the inferior petrosal sinus. Schematic redrawing of the seven drainage patterns described by Mitsuhashi et al. (2007) for the caudal end of the inferior petrosal sinus (IPS). The black structure represents the usual sigmoid sinus–jugular bulb–internal jugular vein (IJV) pathway. Coloured lines indicate the alternative IPS termination patterns, keyed in the figure and defined in Table 3. The anterior condylar vein (ACV) is shown where it participates in the IPS–IJV/VVP transition. The classification concerns IPS drainage, not a morphological classification of the anterior condylar confluence

The long inferior petrosal sinus

A subset of IPS variants is characterised by a long extracranial segment that descends alongside the IJV before terminating. This pattern was first documented by 19th-century anatomists: Knott (1881) observed that 13 of 22 IPSs terminated at or slightly below the lower margin of the jugular foramen, with a maximal extracranial length of approximately 10 mm (Knott 1881). Charpy and Hovelacque (1920, cited in Gailloud et al. 1997) reported extracranial segments varying, when present, between 6 and 30 mm (Charpy and Hovelacque 1920). Labalette (1891, cited in Gailloud et al. 1997) described a venous connection from the intraforaminal IPS to the IJV segment immediately below the JB measuring 4–5 cm (Labalette 1891).

Gailloud et al. (1997) provided the first systematic modern description, reporting an extracranial IPS extension measuring up to 40 mm bilaterally in one anatomical specimen, with the sinus running parallel to the upper IJV before rejoining it. The opening of the IPS into the IJV was avalvular. In four of 100 consecutive cerebral angiograms, a similar variant was observed unilaterally. The authors proposed the term ‘accessory internal jugular vein’ for this extracranial extension and suggested it may provide an alternate endovascular access to the IPS.

Zhang et al. (2010b), in a dedicated MSCT study of long IPSs in 12 sides, reported a mean length of 66.2 ± 17.5 mm (range exceeding 60 mm in 8 sides, with a peak value of 100 mm) (Zhang et al. 2010b). Zhang et al. (2010a), in a larger series of 120 patients (239 sides), found that the IPS extracranial length exceeded 40 mm in ten sides, with the lowest termination level at the inferior margin of the C4 vertebra (Zhang et al. 2010a).

Two recent CT angiographic reports expand the long-IPS spectrum beyond a simple low extracranial termination. Dincă et al. (2025) documented bilateral long IPSs in a 63-year-old male: the two sinuses differed fourfold in length (Table 3), the right being joined below the jugular foramen by the lateral condylar vein. On both sides, the long IPS and the adjacent IJV were applied to, and compressed against, the anterior aspect of the C1 transverse process within the styloid process-C1 nutcracker. This observation is clinically important because a long IPS lying beside the IJV may be compressed within the same osteoligamentous bottleneck and may therefore fail as a collateral or endovascular passage when the IJV itself is compromised (Dinca et al. 2025).

Rusu et al. (2025a) documented a distinct left-sided long extracranial IPS in a 45-year-old female. The 5.55 cm extracranial segment (Table 3) was fenestrated and communicated with the parapharyngeal plexus. The IPS and IJV therefore mimicked a high parapharyngeal duplication of the IJV. Still, the separate skull-base origins distinguished the channels: the IJV continued the SS through the posterolateral jugular foramen, whereas the long IPS exited through the anteromedial jugular foramen and connected to the cavernous-sinus route. This case adds two specific risk

Table 3 Reported anatomical variations of the inferior petrosal sinus and of its caudal termination

Classification or variant	Unit of analysis	Types and reported frequency	Material	Comment
Shiu et al. (1968)	Patient (classified by the dominant side)	I 45%; II 24%; III 24%; IV 7%	57 cavernous sinus venograms from 100 consecutive studies	The four figures already total 100%, although 4% are separately reported as not classifiable; rates are not comparable with per-side series
Miller et al. (1993)	Each IPS–IJV junction separately	I 19.8%*; II 46.3%; III 33.6%; IV 0.4%	268 junctions in 135 consecutive subjects	*Printed as 9.8% in Table 1 of the source; 53/268 = 19.8%. Anatomy symmetrical in only 65% of subjects
Miller et al. (1993)—incomplete type IV	IPS	7 of 268 IPSs (2.6%); 6 of 133 subjects (4.5%)	Same series	very narrow channel from the IJV to the IPS–VVP anastomosis, with normal-calibre IPS beyond
Mitsuhashi et al. (2007)	Side	A 1.2%; B 34.9%; C 37.3% (C-1 23/31, C-2 8/31); D 6.0%; E 3.6%; F 16.9%	83 sides in 63 patients, 3D rotational venography	The only classification that resolves the level of the caudal IPS–IJV junction; type F denotes an absent IPS with a dominant pterygoid plexus
Gailloud et al. (1997)—long extracranial extension	Specimen and angiogram	bilateral in one specimen (40 mm right–left 38 mm); unilateral in 4 of 100 consecutive angiograms	One 85-year-old cadaver plus 100 consecutive cerebral angiograms	Proposed as the "accessory internal jugular vein"; anatomically the ancestor of Mitsuhashi type C
Dinca et al. (2025)—bilateral long IPSs entering the jugular nutcracker	Patient/side	right IPS 1.25 cm long, 0.20 cm diameter; left IPS 5.15 cm long, 0.32 cm diameter; both adjacent to the IJV and compressed at the C1-styloid process level	One 63-year-old male, CT angiography with multiplanar and 3D volume-rendered analysis	Shows that a long IPS may be compressed together with the IJV and may not remain a safe collateral or endovascular route; right IPS joined by the LCV, left IPS descending anteromedially to the IJV
Rusu et al. (2025a)—fenestrated long extracranial IPS	Patient/side	left extracranial IPS 5.55 cm long; fenestration 9.01 mm long / 2.31 mm wide; ACV joined the IPS immediately inferior to the jugular foramen	one 45-year-old female, CT angiography with 2D reconstructions and 3D volume rendering	first reported fenestration of an extracranial IPS; may mimic high IJV duplication unless the separate skull-base origins of the IPS and IJV are traced
Doppman et al. (1999)—hypoplastic or atrophic IPS	Patient	unilateral or bilateral in 25%; bilaterally small in 7%	Large petrosal sampling series	A hypoplastic or plexiform IPS (Miller type III) may cause false-negative petrosal sinus sampling
Benndorf and Campi (2002)—aberrant IPS with low extracranial termination	Patient	Approximately 1%	Reported against the 135-subject Miller series	Single case description; the frequency is an estimate, not a measured prevalence
Raghuram et al. (2018)—MRI visibility and drainage	IPS	91% grade 2 or 3; 65% "typical" type A drainage directly into the IJV	148 IPSs on contrast-enhanced T1	Non-invasive grading; not equivalent to the venographic type systems above
Ekanem et al. (2022)—osseous groove of the IPS	Side	Types I–V; incomplete tunnel 2.5%, complete tunnel 1.0%; larger grooves right-sided in 70%	Dry skull series	Bony rather than venous variation; relevant to the far-lateral and transjugular corridors

Reported frequencies are descriptive and should not be compared directly across rows, because populations, imaging techniques, anatomical definitions and units of analysis differ; numerators and denominators are given where the source reports them

The unit of analysis differs between series and is not interchangeable: Shiu classified patients by the dominant side, whereas Miller and Mitsuhashi classified each side separately. Miller further argued that typing these variants by the calibre of the anterior condylar vein is an oversimplification, because other named and unnamed channels connect the IPS to the VVP and any of them may be dominant in a given patient

morphologies to the long-IPS subgroup: an extracranial IPS fenestration and an imaging mimic of high IJV duplication (Rusu et al. 2025a).

Variation in the caudal course of the IPS directly affects ACC configuration and endovascular accessibility (Gailloud et al. 1997; Rusu et al. 2025a).

The inferior petro-occipital vein

The inferior petro-occipital vein (IPOV; also termed the inferior petroclival vein in parts of the literature) is an extracranial vein that runs along the petro-occipital suture (fissure petrooccipitalis), parallel to but separated from the overlying IPS by a thin plate of bone (Tubbs et al. 2014; Matsuo et al. 2021). The vein connects the ACC at its caudal pole to the venous plexus of Rektorzik (VPR) at its cranial pole, the latter situated at the exit of the carotid canal at

the petrous apex, adjacent to the foramen lacerum. This craniocaudal orientation, ascending beneath the petro-occipital suture from the anterior condylar fossa towards the petrous apex and foramen lacerum, is the topographic basis for the designation 'petro-occipital' adopted here (Section "Terminology and conventions"). Since the VPR, in turn, communicates with the CS in approximately 89% of cases (Imai et al. 2022), the IPOV represents an indirect extracranial venous corridor linking the ACC–at the level of the HC–to the CS through the petrous apex and foramen lacerum. It was described by Trolard (1868) as connecting the internal carotid artery venous plexus (of Rektorzik) to the ACC and the JB region (Trolard 1868; San Millán Ruíz et al. 2002; Spittau et al. 2015). In the classical French anatomical tradition, this structure was designated the 'sinus pétro-occipital d'Englisch' by Paturet (1958), a term that records its early recognition as a channel distinct from the dural IPS (Paturet 1958).

Tubbs et al. (2014) identified the IPOV in 83.3% of 24 cadaveric sides (20 of 24), noting that it typically connected the internal carotid venous plexus to the superior JB. On 10% of sides, the anterior part communicated directly with the CS; on 15%, the posterior vein drained into the IPS at its termination. The IPOV was usually larger when a nondominant transverse sinus was present, and the IPS tended to be smaller when an underlying IPOV was present. On 20% of sides, the posterior aspect communicated with the HC veins, and diploic veins from the clivus drained into the IPOV on three sides (Tubbs et al. 2014).

Matsuo et al. (2021) found that the IPOV (termed 'inferior petroclival vein' in their study) was identifiable on all 51 radiologically examined sides. Its rostral end connected to the carotid artery venous plexus, and its caudal end drained into the IPS (96.1%) or directly into the ACV (3.9%) (Matsuo et al. 2021). The IPOV has been used as an alternative transvenous route to the cavernous sinus (Kurata et al. 2012) and is relevant to endoscopic skull-base surgery (Mizutani et al. 2018b).

Evidence for communication between the IPS and the IPOV is scattered but real. Direct anatomical evidence was provided by Tubbs et al. (2014), who found small venous connections between the IPOV and the overlying IPS in 40% of cadaveric sides (Tubbs et al. 2014). Mizutani et al. (2017) further demonstrated, using CT-DSV, that clival emissary veins may connect the IPS with the IPOV in the middle clivus (Mizutani et al. 2017). The small IPOV–IPS connections seen at dissection by Matsuo et al. (2021) are consistent with these observations (Matsuo et al. 2021). Thus, IPS–IPOV communication may occur either directly through small transosseous channels, indirectly through clival emissary/diploic veins, or functionally through the ACC/petrosal confluence. The vein is shown with the intrapetrous vein and the IPS in Fig. 7, and its direct anastomosis with the IPS in Fig. 4.

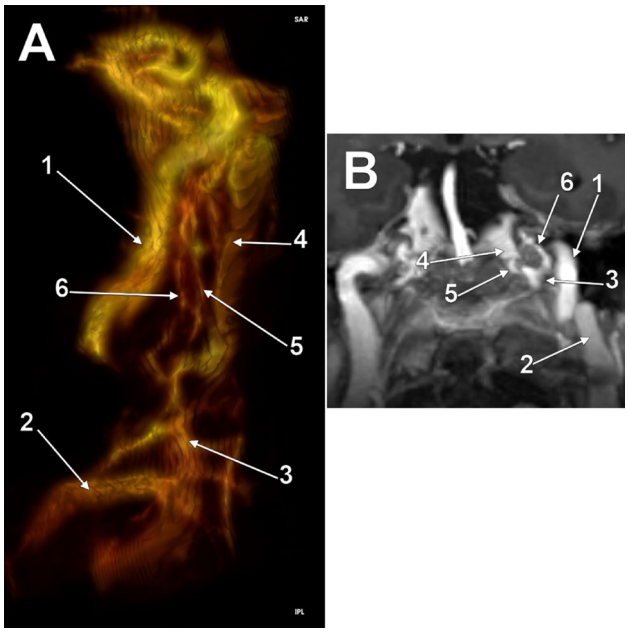


Fig. 7 The intrapetrous vein, the inferior petro-occipital vein and the inferior petrosal sinus. MR angiogram. Left side. **A** Three-dimensional volume rendering, postero-superior view. **B** coronal curved-planar slice. 1. internal carotid artery; 2. internal jugular vein; 3. anterior condylar confluence; 4. inferior petrosal sinus; 5. inferior petro-occipital vein; 6. intrapetrous vein

The internal carotid artery venous Plexus (Plexus of Rektorzik)

The venous plexus of Rektorzik (VPR), first described by Rektorzik in 1858 (Imai et al. 2022; Skrzat and Goncerz 2023), is a network of small valveless veins surrounding the internal carotid artery (ICA) as it traverses the carotid canal within the petrous temporal bone (Cironi et al. 2022; Imai et al. 2022; Skrzat and Goncerz 2023). In French classical anatomical nomenclature, Paturet (1958) referred to this structure as the 'sinus carotidien de Rektorzik' (Paturet 1958). The plexus connects superiorly to the CS and inferiorly to the ACC via the IPOV (Paturet 1958; San Millán Ruíz et al. 2002; Imai et al. 2022).

Imai et al. (2022) conducted the first CT-digital subtraction venography (CT-DSV) study specifically targeting the VPR in 253 patients. Key findings included: the VPR was identified in 60 patients (24%, or 71 of 506 sides = 14%); it was significantly more common on the right side than the left (50 vs. 21, $p = 0.0002$); the mean age was significantly lower in patients with VPR than in those without (53 vs. 57 years, $p = 0.02$).

Venous connections of the VPR. Distally, the CS was the most frequent connection (63 of 71 VPRs, 89%), followed

by the IPOV and clival diploic vein. Most VPRs (49 of 71) were connected to both the CS and IPOV. Proximally, the VPR exiting the outer orifice of the carotid canal and heading medially emptied mainly into the ACC (27 of 71, 38%). More than half of the VPRs (42 of 71) had no identifiable proximal connections and radiologically appeared as blind alleys (Imai et al. 2022). Based on these findings, Imai et al. (2022) proposed a direct venous connection between the proximal VPR and the ACC. The confluence, the plexus of Rektorzik and the inferior petro-occipital vein are seen together in the axial plane in Fig. 8.

Skrzat and Goncerz (2023) described the VPR as a longitudinal venous pathway with an anterosuperior connection to the CS and a posteroinferior connection to the IJV, a configuration reported to be more conspicuous in fetuses than in adults. They also treated the IPOV/inferior petroclival vein as a separate channel that may receive branches from the VPR and convey them toward the ACC, superior JB or IJV (Skrzat and Goncerz 2023). This distinction is supported by Mizutani et al. (2018b), who described both one or a few extracranial VPR-IJV channels and, separately, a VPR-inferior petroclival vein connection at the foramen lacerum (Mizutani et al. 2018b). The posteroinferior connection in Skrzat and Goncerz (2023) should therefore not be identified automatically with the IPOV of Englisch.

Transpetrous connections of the plexus have also been described (Sepulveda et al. 2015). In the cadaveric study of Couldwell et al. (2021), transosseous temporal veins were present on all 20 sides examined, with one to six per side and a calibre of 0.6–1.1 mm, connecting the petrosal sinuses, the IPOV, the basilar plexus and transclival veins, and communicating with the internal carotid venous plexus on 70% of sides (Couldwell et al. 2021). The ACC was not demonstrated as an endpoint.

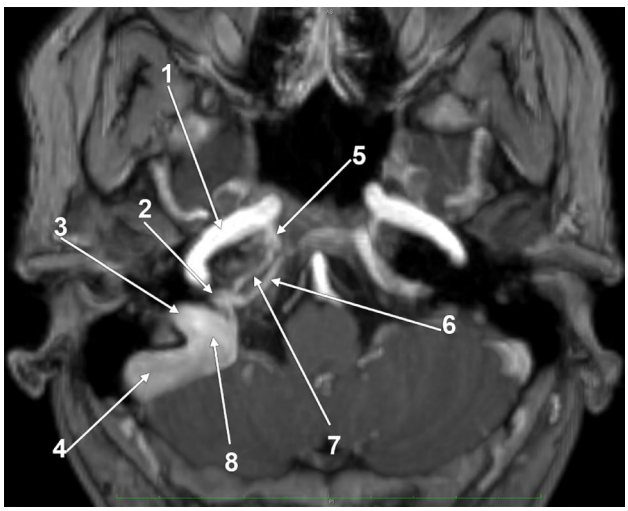


Fig. 8 The venous anatomy antero-medial to the initial segment of the internal jugular vein. MR angiogram. Curved-planar axial slice. Right side. 1. internal carotid artery; 2. anterior condylar confluence; 3. internal jugular vein; 4. sigmoid sinus; 5. venous plexus of Rektorzik; 6. inferior petrosal sinus; 7. inferior petro-occipital vein of Trolard; 8. jugular bulb. The confluence is seen in the axial plane with the plexus of Rektorzik antero-superior to it and the inferior petro-occipital vein passing medially

Imai et al. (2022) discussed the physiological significance of the VPR, proposing that it buffers the ICA within its bony canal and forms part of the skull base venous reservoir that stabilises venous and intracranial pressures during postural changes (Imai et al. 2022). The discrepancy between VPR prevalence in cadaveric studies, which approaches 100%, (Cironi et al. 2022) and in CT-DSV (24%) is best explained by the fact that pressurised injection of dye in cadavers may open venous channels that are physiologically closed or have only stagnated flow (Imai et al. 2022). The difference illustrates the distinction between anatomical constancy and imaging visibility drawn in Section "Terminology and conventions".

The prevertebral venous plexus

The prevertebral venous plexus, located on the anterior aspect of the atlanto-occipital membrane, provides a direct connection between the ACC and the anterior external VVP (AEVVP). This tributary was one of the six regular contributors to the ACC identified by San Millán Ruíz et al. (2002).

Yamada et al. (2022) provided the most detailed investigation of this previously under-studied venous territory using CT-DSV in 273 patients (ages 6 months to 93 years). Key findings included: the prevertebral vein was present on about half of the sides (Table 1) and bilaterally in 132 cases (48%); the cranial connection was mostly with the ACC (95% on both sides), with minor connections to the ACV (1–3%), IPS (1–2%), or inferior petro-occipital vein (IPOV) (1–3%); the bilateral prevertebral veins fused in the midline at the junction between the occipital bone and the first cervical vertebra in 115 cases (42%), giving the veins a "necklace" appearance (Yamada et al. 2022).

Caudal connections of the prevertebral vein. More than half of the prevertebral veins had no caudal connection; the remainder joined the AEVVP (22–26%), a vein around the odontoid process (16%) or, rarely, clival diploic veins (Yamada et al. 2022). Patients with a prevertebral vein were significantly younger than those without, as for the VPR (Section "The Internal Carotid Artery Venous Plexus (Plexus of Rektorzik)").

The odontoid vein–a novel finding. Yamada et al. (2022) identified a previously unrecognised venous structure near the tip of the odontoid process in 10% of all cases (27 of 273 patients). This vein or venous plexus, located between the odontoid process and the lower end of the clivus, connected to the prevertebral vein (85–89%), AIVVP (70–74%),

AEVVP (15–37%), and clival diploic veins (4–7%). Because the prevertebral vein runs along the anterior aspect of the occipital condyles rather than along the anterior surface of the vertebral body, Yamada et al. (2022) proposed that 'precondylar vein' may be a more appropriate name than 'prevertebral vein'. Similarly, they proposed 'odontoid vein' for the structure near the odontoid process.

The connection of the plexus with both confluences is shown in Fig. 9, its relation to the posterior fossa veins in Fig. 10, and its vein-plexus-vein morphology at the level of the atlas in Fig. 2.

The posterior condylar vein

The PCV was present in 79% of sides (19 of 24) in the corrosion cast study. Its diameter was usually larger than that of the ACV. It generally took its origin from the superior bulb of the IJV, although it was seen to arise from the medial side of the distal portion of the SS on one occasion. It drained into the deep cervical vein and also communicated with the horizontal portion of the VAVP (San Millán Ruíz et al. 2002).

The PCV is the most variable of the condylar veins, showing greater variation in size and symmetry than any other craniocervical venous structure (Caruso et al. 1999; Takahashi et al. 2005); the reported prevalences are collected in Table 1. Two concordant classifications of its intracranial termination exist. Matsushima et al. (2014) identified posterior condylar canals on 82 of 100 CT sides and classified their courses as SS, JB, occipital sinus, and anterior condylar emissary vein types (Matsushima et al. 2014). Ota et al. (2017) applied the same four categories intraoperatively in 52 transcondylar fossa approaches (104 sides), with the distribution given in Table 1 (Ota et al. 2017). Clinically, an enlarged PCV may cause pulsatile tinnitus, and its ligation may result in venous ischaemia, so the vessel should be reported preoperatively (Pekçevik and Pekçevik 2014). Embryologically, the ACV and PCV are among the first emissary veins to appear, from the third fetal month, the ACV before the PCV (Okudera et al. 1994).



Fig. 9 The craniovertebral region and the prevertebral plexus. CT angiogram, three-dimensional volume rendering. Anterior view. The prevertebral vein or plexus (arrowheads) is connected with the anterior condylar confluences on both sides (arrows)

Matsushima et al. (2014) further separated bony-canal recognition from venous opacification: PCCs were identified on 82/100 CT sides, whereas a PCEV was enhanced on 73/100 sides. Among the 73 opacified PCEVs, 67% were jugular-bulb type, 29% sigmoid-sinus type and 4% occipital-sinus type; the anterior-condylar-emissary-vein type was absent on CT but occurred in 3% of dry-skull PCCs. The authors considered supine, jugular-dominant flow a possible reason for non-opacification, again cautioning against equating invisibility with absence.

The anterior condylar emissary vein type deserves separate mention, because it is the only configuration in which the two condylar canals communicate directly: the PCV, within the posterior condylar canal, joins the anterior condylar vein within the HC intracranially, without an intervening sinus or bulb. Its reported frequency differs by more than twofold between the two series, 3% of dry-skull canals for Matsushima et al. (2014) against 7.7% of operative sides for Ota et al. (2017), and it was not opacified on CT venography in any case, so that both figures may understate it (Matsushima et al. 2014; Ota et al. 2017). It is the anatomical basis on which a shunt of the posterior condylar canal may drain by way of the confluence.

The marginal sinus

The MS is an intracranial dural venous sinus that surrounds the foramen magnum. San Millán Ruíz et al. (2002) noted the MS in 83.3% of their corrosion casts (10 of 12 cases). It connected anteriorly with the ACV in all cases, and on one occasion it bridged the ACV with a suboccipital vein. Tubbs et al. (2006) examined the MS in 15 cadavers and found its maximal vertical height ranged from 7 to 15 mm (mean 10 mm), with 93% demonstrating significant drainage into the veins of the HC, thereby communicating with the ACC. Communication with the basilar venous plexus occurred in 80%, and with the occipital sinus in 100%.

Posteriorly, the MS may connect with the veins of the suboccipital region or represent the major drainage pathway of a persistent occipital sinus (Spittau et al. 2015). Tubbs et al. (2018) further showed that the anterior internal vertebral plexus connected to the anterior half of the MS in 33% and to the anterolateral parts in 20%, while the posterior internal venous plexus connected to the posterior MS in 80% of specimens (Tubbs et al. 2018). These connections are clinically relevant for foramen magnum surgery and for understanding compensatory venous drainage in cases of transverse sinus aplasia or hypoplasia (Radoi et al. 2022).

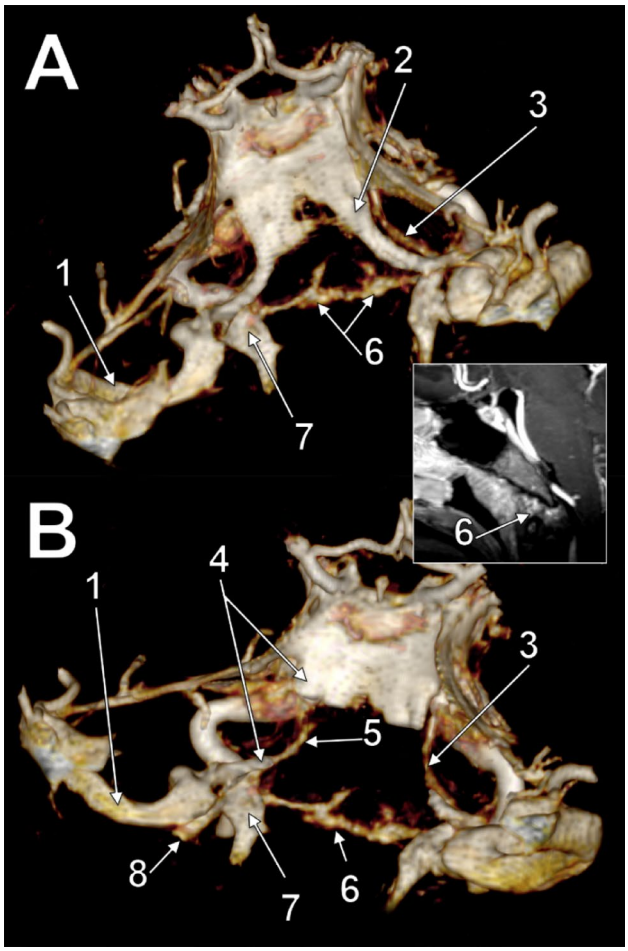


Fig. 10 The prevertebral plexus in relation to the posterior fossa veins. MR angiogram. A: three-dimensional volume rendering of the posterior fossa veins, postero-superior view, inferior petrosal sinuses retained. B: the same, posterior view, with the left inferior petrosal sinus suppressed from the rendering. Inset: curved-planar medio-sagittal slice. 1. left sigmoid sinus; 2. right inferior petrosal sinus; 3. right inferior petro-occipital vein; 4. left inferior petrosal sinus, excluded from the reconstruction; 5. left inferior petro-occipital vein; 6. prevertebral plexus; 7. left anterior condylar vein; 8. left posterior condylar vein

The MS is shown in continuity with the internal VVP and the anterior condylar veins in Fig. 11.

The clival diploic veins

Clival diploic veins (CDVs) are intraosseous venous channels within the clivus that provide additional, less constant connections to the ACC. Mizutani et al. (2017) identified CDVs in 14.0% of 50 CT-DSV cases. Half of the emissary veins identified connected the IPS with the IPOV in the middle clivus. The CDV was connected superiorly to the posterior intercavernous sinus or the rostral end of the basilar plexus, and inferiorly to the IPOV, ACV, MS, or the

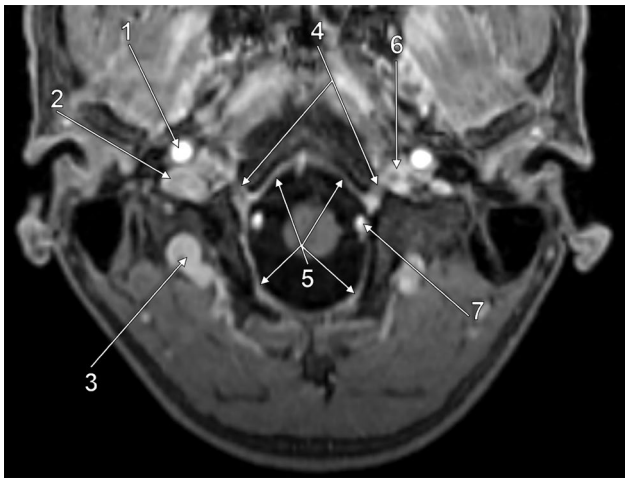


Fig. 11 The marginal sinus and internal vertebral venous plexus complex. MR angiogram. Curved-planar axial slice. 1. right internal carotid artery; 2. right internal jugular vein; 3. right posterior condylar vein connecting to the SCS; 4. anterior condylar veins; 5. marginal sinus; 6. left anterior condylar confluence, plexiform, with a ring-like appearance in this plane; 7. left vertebral artery

ACC. The CDV was more frequent in patients with a preselar type of clivus (42.9%) (Mizutani et al. 2017).

These intraosseous venous pathways are relevant for endonasal endoscopic skull base surgery, where clival bone drilling may breach these channels (Mizutani et al. 2018b).

Triantafyllou et al. (2025) described another rare intraosseous variant: an accessory emissary foramen measuring 1.59 × 2.87 mm in the anterior paracondylar region, located inferior to the inferior petrosal sinus groove, identified in a single dried skull. Its position and trajectory suggest it transmits an emissary vein that directly connects the IPS with the ACC via a novel bony channel. Triantafyllou et al. (2025) proposed the name ‘far anterior paracondylar foramen’ for this structure. Although observed in a single specimen, such a channel could be an alternative IPS-to-ACC route or a source of unexpected bleeding during drilling at the petroclival fissure.

Functional and surgical significance

Postural venous haemodynamics

The ACC plays a central role in the physiological switching of cerebral venous drainage from the jugular system (dominant supine) to the vertebral venous system (dominant upright). At the systemic level, this postural switch was quantified by Valdueza et al. (2000), who showed by duplex sonography that jugular predominance is confined to the supine position, with the vertebral venous system becoming the principal outflow route in the erect position (total

jugular flow falling from approximately 700 to 70 mL/min between 0° and 90° of body elevation, while vertebral flow rose from 40 to 210 mL/min) (Valdueza et al. 2000). At the craniocervical junction, Kosugi et al. (2020) demonstrated that from supine to upright posture, IJV cross-sectional area decreases by approximately 70–78%, while the ACV cross-sectional area increases by 110–144%. The ACC becomes more prominent, identifying the ACV as the condylar channel that mediates this diversion into the vertebral system (Kosugi et al. 2020).

Surgical and endovascular implications

Knowledge of the ACC is essential during far-lateral, transcondylar, and endoscopic skull base surgical approaches. The LCV serves as a route for transvenous access during endovascular procedures and may also need to be obliterated (Matsushima et al. 2015; Hellstern et al. 2019). The posterior condylar emissary vein (PCEV), encountered during transcondylar fossa approaches, must be managed based on preoperative CT venography of its drainage pattern to avoid inadvertent sinus injury (Ota et al. 2017). The MS is at risk during foramen magnum approaches, and its connections with the ACC must be preserved to avoid compromising cerebral venous drainage (Tubbs et al. 2006, 2018). Detailed knowledge of the IPS anatomy at its junction with the jugular foramen, including its frequent extracranial termination below the skull base, is critical for catheter navigation during petrosal sinus sampling and transvenous embolisation (Rubinstein et al. 1995). The prevertebral venous network described by Yamada et al. (2022) may be encountered during ventral craniocervical surgical approaches, and the VPR may be encountered during transnasal endoscopic procedures exposing the petrous ICA (Imai et al. 2022). Payman et al. (2022) detailed the condylar venous anatomy met in each modification of the far-lateral approach: the transcondylar approach, through the posterior third of the condyle, is limited anteriorly by the HC, whose venous plexus is the landmark at which drilling stops; the supracondylar approach, through the jugular tubercle, may bleed copiously from the posterior condylar emissary veins; and the paracondylar approach, through the jugular process, is bounded by the lateral and posterior condylar veins, whose courses should be assessed preoperatively (Payman et al. 2022). Sreenivasan et al. (2022) demonstrated that abnormal communication between the PCC and HC, a variant identifiable on preoperative CT, requires modified drilling trajectories (cranial and lateral rather than caudal and medial) to avoid avulsion of the hypoglossal venous plexus and potential torrential bleeding. These studies confirm that no single anatomical template can be assumed for the condylar venous system (Ota et al. 2017; Lucena et al. 2025). Patient-specific preoperative imaging is mandatory for safe surgical planning.

Because the confluence is reached more readily from the venous side than from the arterial side, transvenous embolisation is the established first-line technique for shunts at the ACC and within the HC, and the anatomy set out above determines which corridor is available: the IJV and JB in most cases, the IPS where its caudal termination permits catheterisation, and the LCV or the IPOV when the jugular route is occluded (Spittau et al. 2015; Hellstern et al. 2019). The arterial route is used more selectively, because the feeding branches are small and carry dangerous anastomoses to the vertebrobasilar circulation, and because liquid embolic agents injected from the arterial side risk lower cranial nerve palsy (Takemoto et al. 2014). Coil packing within the HC carries a further hazard specific to this site: mechanical compression of the hypoglossal nerve, which shares the canal with the ACV.

The venous structures surrounding the third segment of the vertebral artery were named the suboccipital cavernous sinus (SCS) by Arnautovic et al. (1997), and the same compartment is also described as the suboccipital venous plexus; it is the extracranial territory into which the PCV drains (Arnautovic et al. 1997; Takahashi et al. 2005). Both terms should be searched when the posterior condylar route is assessed before surgery or transvenous embolisation.

Limitations

The evidence collated here is heterogeneous. Corrosion casts, dissection, CT, CTA, MR imaging, CT-DSV, catheter venography and operative observation do not detect the same channels with the same sensitivity: pressurised injection opens channels that are collapsed in life, whereas a supine contrast-enhanced acquisition may fail to opacify a channel in which flow is reversed or stagnant, so that reported frequencies partly measure the method rather than the anatomy. Denominators differ between studies: casts, specimens, sides, IPS–IJV junctions, or patients; patient-based series may classify by the dominant side. Venous calibre and drainage direction change with posture, and almost all imaging data were acquired supine. The mapping of historical terms onto modern nomenclature is in places uncertain, notably for the sinus pétro-occipital d'Englisch, the inferior petro-occipital and petroclival veins, and the suboccipital cavernous sinus and venous plexus, so that some discordance between sources may be terminological rather than anatomical. We retrieved the literature systematically, but did not triage independently in duplicate, perform a risk-of-bias assessment, or assess study quality; the published record is likely to over-represent unusual variants and clinically relevant cases, as the single-case reports of

long, fenestrated, or compressed sinuses illustrate. Finally, the angiographic material was selected for illustration from anonymised institutional archives and is neither consecutive nor demographically characterised; it shows that the described configurations exist and how they appear on MR and CT angiography, but it cannot be used to estimate their frequency. The IPS–IJV ring in particular is a descriptive term for an appearance already depicted in the multislice CT series discussed in Section "General anatomy of the ACC", not a new entity.

Conclusion

The anterior condylar confluence is a small, valveless venous hub at the external orifice of the hypoglossal canal. It links the dural sinuses of the posterior fossa, the internal jugular vein and the vertebral venous system, and cerebral venous outflow is redirected through it with changes of posture. The channels that join it, namely the anterior, lateral and posterior condylar veins, the bridging veins from the jugular bulb, the inferior petrosal sinus, the inferior petro-occipital vein with the plexus of Rektorzik, the prevertebral plexus, the marginal sinus and the clival diploic veins, vary individually in presence, calibre, course and termination, and their reported frequencies depend on the method and on the unit of analysis as much as on the anatomy. Recognition of this variability on patient-specific imaging, rather than reliance on any single template, is what makes the confluence safe to traverse in far-lateral and transcondylar surgery, to catheterise for transvenous access to the cavernous sinus and to the confluence itself, and to interpret when a dural arteriovenous fistula of the region is localised and treated.

Supplementary Information The online version contains supplementary material available at https://doi.org/10.1007/s12565-026-00974-2.

Author contributions MCR: Conceptualization, Data curation, Investigation, Software, Writing – original draft, Writing – review & editing. AMJ: Validation, Resources, Methodology, Writing – review & editing. PMR: Visualization, Project administration, Software. RCT: Investigation, Visualization, Writing – review & editing.

Funding This research received no specific grant from public, commercial, or not-for-profit funding agencies.

Data availability No datasets were generated or analysed during the current study.

Declarations

Conflict of interest The authors declare no competing interests.

Ethical approval The research was conducted in accordance with the Declaration of Helsinki. The study was approved by the Ethics Committee of the Municipal Emergency Clinical Hospital of Timişoara (approval no. E−4247/15.10.2025).

Open Access This article is licensed under a Creative Commons Attribution 4.0 International License, which permits use, sharing, adaptation, distribution and reproduction in any medium or format, as long as you give appropriate credit to the original author(s) and the source, provide a link to the Creative Commons licence, and indicate if changes were made. The images or other third party material in this article are included in the article's Creative Commons licence, unless indicated otherwise in a credit line to the material. If material is not included in the article's Creative Commons licence and your intended use is not permitted by statutory regulation or exceeds the permitted use, you will need to obtain permission directly from the copyright holder. To view a copy of this licence, visit http://creativecommons.org/licenses/by/4.0/.

References

Arnautovic KI, Al-Mefty O, Pait TG, Krisht AF, Husain MM (1997) The suboccipital cavernous sinus. J Neurosurg 86:252–262

Benndorf G, Campi A (2002) Aberrant inferior petrosal sinus: unusual transvenous approach to the cavernous sinus. Neuroradiology 44:158–163

Caruso RD, Rosenbaum AE, Chang JK, Joy SE (1999) Craniocervical junction venous anatomy on enhanced MR images: the suboccipital cavernous sinus. AJNR Am J Neuroradiol 20:1127–1131

Charpy A, Hovelacque A (1920) Veines. In: Nicolas A (ed) Traité d'Anatomie Humaine de Poirier et Charpy, 3rd edn. Masson, Paris

Choi JW, Kim BM, Kim DJ, Kim DI, Suh SH, Shin NY et al (2013) Hypoglossal canal dural arteriovenous fistula: incidence and the relationship between symptoms and drainage pattern. J Neurosurg 119:955–960

Cironi K, Wang C, Iwanaga J, Lockwood J, Mathkour M, Bui CJ et al (2022) Anatomical study of the internal carotid venous plexus: new findings with application to skull base surgery. Acta Neurochir (Wien) 164:1923–1928

Couldwell MW, Jackson N, Wysiadecki G, Keen J, Iwanaga J, Delashaw J et al (2021) Transosseous veins of the temporal bone: connection between middle and posterior cranial fossa venous structures. World Neurosurg 155:e824–e829

Dinca V, Ionescu P, Tudose RC, Munteanu M, Vrapciu AD, Rusu MC (2025) Anatomical Reasons for an Impaired Internal Jugular Flow. Medicina (Kaunas) 61:1627

Doppman JL, Chang R, Oldfield EH, Chrousos G, Stratakis CA, Nieman LK (1999) The hypoplastic inferior petrosal sinus: a potential source of false-negative results in petrosal sampling for Cushing's disease. J Clin Endocrinol Metab 84:533–540

Ekanem UI, Olewnik L, Porzionato A, Macchi V, Iwanaga J, Loukas M et al (2022) Morphology of the groove of the inferior petrosal sinus: application to better understanding variations and surgery of the skull base. Anat Cell Biol 55:135–141

Gailloud P, Fasel JH, Muster M, Desarzens F, Ruefenacht DA (1997) Termination of the inferior petrosal sinus: an anatomical variant. Clin Anat 10:92–96

Hellstern V, Aguilar-Perez M, Schob S, Bhogal P, Almatter M, Kurucz P et al (2019) Endovascular treatment of dural arteriovenous fistulas of the anterior or posterior condylar vein: a cadaveric and clinical study and literature review. Clin Neuroradiol 29:341–349

Iampreechakul P, Wangtanaphat K, Chuntaroj S, Khunvutthidee S, Wattanasen Y, Hangsapruek S et al (2025) Dural arteriovenous fistulas of the anterior condylar confluence involving the anterior

condylar vein within the hypoglossal canal: two case reports. Surg Neurol Int 16:69
Imai R, Mizutani K, Akiyama T, Horiguchi T, Takatsume Y, Toda M (2022) Imaging of the venous plexus of Rektorzik using CT-digital subtraction venography: a retrospective study. Neuroradiology 64:1961–1968
Katsuta T, Rhoton AL Jr, Matsushima T (1997) The jugular foramen: microsurgical anatomy and operative approaches. Neurosurgery 41:149–201 (**discussion 201-142**)
Knott JF (1881) On the cerebral sinuses and their variations. J Anat Physiol 16:27–42
Kosugi K, Yamada Y, Yamada M, Yokoyama Y, Fujiwara H, Yoshida K et al (2020) Posture-induced changes in the vessels of the head and neck: evaluation using conventional supine CT and upright CT. Sci Rep 10:16623
Kurata A, Suzuki S, Iwamoto K, Nakahara K, Inukai M, Niki J et al (2012) A new transvenous approach to the carotid-cavernous sinus via the inferior petrooccipital vein. J Neurosurg 116:581–587
Labalette F (1891) Les veines de la tête et du cou. Thèse de Lille, Faculté de Médecine de Lille
Loukas M, Shea M, Shea C, Lutter-Hoppenheim M, Zand P, Tubbs RS et al (2010) Jean Baptiste Paulin Trolard (1842-1910): his life and contributions to neuroanatomy. J Neurosurg 112:1192–1196
Lucena GMO, Lemos GJP, Araújo LSMP, Alencar MS, Martins ACA, Martins C (2025) Posterior condylar canal: anatomy and medical insights. Neurol Surg Anat 2:1–12
Matsuo S, Komune N, Amano T, Nakamizo A (2021) Microsurgical anatomy of the inferior petroclival vein and its relation to surrounding structures: a cadaveric and radiological study. Oper Neurosurg 21:E83–E88
Matsushima K, Kawashima M, Matsushima T, Hiraishi T, Noguchi T, Kuraoka A (2014) Posterior condylar canals and posterior condylar emissary veins-a microsurgical and CT anatomical study. Neurosurg Rev 37:115–126
Matsushima K, Funaki T, Komune N, Kiyosue H, Kawashima M, Rhoton AL Jr (2015) Microsurgical anatomy of the lateral condylar vein and its clinical significance. Neurosurgery 11(Suppl 2):135–145 (**discussion 145-136**)
Miller DL, Doppman JL, Chang R (1993) Anatomy of the junction of the inferior petrosal sinus and the internal jugular vein. AJNR Am J Neuroradiol 14:1075–1083
Mitsuhashi Y, Nishio A, Kawahara S, Ichinose T, Yamauchi S, Naruse H et al (2007) Morphologic evaluation of the caudal end of the inferior petrosal sinus using 3D rotational venography. AJNR Am J Neuroradiol 28:1179–1184
Miyachi S, Ohshima T, Izumi T, Kojima T, Yoshida J (2008) Dural arteriovenous fistula at the anterior condylar confluence. Interv Neuroradiol 14:303–311
Mizutani K (2024) Inferior petrosal sinus and anterior condylar confluence and surrounding venous anatomy. No Shinkei Geka 52:605–616
Mizutani K, Toda M, Kurasawa J, Akiyama T, Fujiwara H, Jinzaki M et al (2017) Analysis of the venous channel within the clivus using multidetector computed tomography digital subtraction venography. Neuroradiology 59:213–219
Mizutani K, Akiyama T, Minami Y, Toda M, Fujiwara H, Jinzaki M et al (2018a) Intraosseous venous structures adjacent to the jugular tubercle associated with an anterior condylar dural arteriovenous fistula. Neuroradiology 60:487–496
Mizutani K, Akiyama T, Yoshida K, Toda M (2018b) Skull base venous anatomy associated with endoscopic skull base neurosurgery: a literature review. World Neurosurg 120:405–414
Mortazavi MM, Tubbs RS, Riech S, Verma K, Shoja MM, Zurada A et al (2012) Anatomy and pathology of the cranial emissary veins: a review with surgical implications. Neurosurgery 70:1312–1318 (**discussion 1318-1319**)
Natsis K, Piagkou M (2015) The anatomical variability of the emissary condylar veins, its identification and clinical significance. J Neurosci Rural Pract 6:123–124
Okudera T, Huang YP, Ohta T, Yokota A, Nakamura Y, Maehara F et al (1994) Development of posterior fossa dural sinuses, emissary veins, and jugular bulb: morphological and radiologic study. AJNR Am J Neuroradiol 15:1871–1883
Ota N, Tanikawa R, Yoshikane T, Miyama M, Miyazaki T, Kinoshita Y et al (2017) Surgical microanatomy of the posterior condylar emissary vein and its anatomical variations for the transcondylar fossa approach. Oper Neurosurg 13:382–391
Paturet G (1958) Traité d'anatomie humaine. Tome III, Fascicule II: Appareil circulatoire (veines), Appareil de la phonation, Appareil respiratoire, Corps thyroïde, Parathyroïdes, Thymus, Médiastin. Masson & Cie, Paris
Payman A, Rios Zermeno J, Hirpara A, El-Sayed IH, Abla A, Rodriguez Rubio R (2022) Immersive surgical anatomy of the far-lateral approach. Cureus 14:e31257
Pekçevik Y, Pekçevik R (2014) Why should we report posterior fossa emissary veins? Diagn Interv Radiol 20:78–81
Radoi PM, Minca DI, Rusu MC, Toader C (2022) Bilateral absence of the transverse sinuses with fenestrated superior sagittal sinus draining through enlarged occipital and marginal sinuses. Folia Morphol (Warsz) 81:781–784
Raghuram K, Durgam A, Sartin S (2018) Assessment of the inferior petrosal sinus on T1-weighted contrast-enhanced magnetic resonance imaging. J Clin Imaging Sci 8:22
Rubinstein D, Burton BS, Walker AL (1995) The anatomy of the inferior petrosal sinus, glossopharyngeal nerve, vagus nerve, and accessory nerve in the jugular foramen. AJNR Am J Neuroradiol 16:185–194
Rusu MC, Dincă V, Tudose RC (2025a) Fenestrated carotid axis at the carotid bifurcation and long inferior petrosal sinus, novel findings. Surg Radiol Anat 47:218
Rusu MC, Tudose RC, Vrapciu AD, Butucescu M (2025b) Details of rare and novel anatomical variations in a case with bilateral long styloid processes. Rom J Morphol Embryol 66:399–403
San Millán Ruíz D, Gailloud P, Rüfenacht DA, Delavelle J, Henry F, Fasel JHD (2002) The craniocervical venous system in relation to cerebral venous drainage. AJNR Am J Neuroradiol 23:1500–1508
Sepulveda I, Schmidt T, Platin E (2015) Intrapetrous anastomosis between the internal jugular vein and the superior petrosal sinus: cone beam computed tomography incidental finding. J Clin Imaging Sci 5:46
Shiu PC, Hanafee WN, Wilson GH, Rand RW (1968) Cavernous sinus venography. Am J Roentgenol Radium Ther Nucl Med 104:57–62
Skrzat J, Goncerz G (2023) The venous plexus of Rektorzik-anatomoclinical issues retrieved from the literature data. Folia Med Cracov 63:5–13
Spittau B, Millan DS, El-Sherifi S, Hader C, Singh TP, Motschall E et al (2015) Dural arteriovenous fistulas of the hypoglossal canal: systematic review on imaging anatomy, clinical findings, and endovascular management. J Neurosurg 122:883–903
Sreenivasan S, Ota N, Noda K, Kinoshita Y, Kamiyama H, Tokuda S et al (2022) Aberrant drainage of posterior condylar emissary vein and abnormal orifice of hypoglossal canal: surgical implications in the transcondylar fossa approach for VA-PICA junction aneurysm. Acta Neurochir (Wien) 164:2119–2126
Suzuki Y, Toma N, Kuroda Y (2020) Dural arteriovenous fistula formation as Eagle jugular syndrome: a case report and literature review. World Neurosurg 144:154–161
Takahashi S, Sakuma I, Omachi K, Otani T, Tomura N, Watarai J et al (2005) Craniocervical junction venous anatomy around the suboccipital cavernous sinus: evaluation by MR imaging. Eur Radiol 15:1694–1700

Takemoto K, Tateshima S, Rastogi S, Gonzalez N, Jahan R, Duckwiler G et al (2014) Onyx embolization of anterior condylar confluence dural arteriovenous fistula. J Neurointerv Surg 6:e13

Tanoue S, Goto K, Oota S (2005) Endovascular treatment for dural arteriovenous fistula of the anterior condylar vein with unusual venous drainage: report of two cases. AJNR Am J Neuroradiol 26:1955–1959

Tanoue S, Kiyosue H, Sagara Y, Hori Y, Okahara M, Kashiwagi J et al (2010) Venous structures at the craniocervical junction: anatomical variations evaluated by multidetector row CT. Br J Radiol 83:831–840

Triantafyllou G, Paschopoulos I, Karangeli N, Tsakotos G, Piagkou M (2025) A unique emissary foramen: the far anterior paracondylar foramen. J Craniofac Surg. https://doi.org/10.1097/scs.0000000000011204

Trolard P (1868) Anatomie du systeme veineux de l'encéphale et du crane. Faculté de Médecine de Paris

Tubbs RS, Ammar K, Liechty P, Wellons JC 3rd, Blount JP, Salter EG et al (2006) The marginal sinus. J Neurosurg 104:429–431

Tubbs RS, Hansasuta A, Loukas M, Louis RG Jr., Shoja MM, Salter EG et al (2007) The basilar venous plexus. Clin Anat 20:755–759

Tubbs RS, Watanabe K, Loukas M, Cohen-Gadol AA (2014) Anatomy of the inferior petro-occipital vein and its relation to the base of the skull: application to surgical and endovascular procedures of the skull base. Clin Anat 27:698–701

Tubbs RS, Demerdash A, Loukas M, Cure J, Oskouian RJ, Ansari S et al (2018) Intracranial connections of the vertebral venous plexus: anatomical study with application to neurosurgical and endovascular procedures at the craniocervical junction. Oper Neurosurg 14:51–57

Tudose RC, Rusu MC, Triantafyllou G, Piagkou M, Toader C, Radoi PM (2024) Anatomical variations of the jugular bulb: a critical and comprehensive review. Medicina (Kaunas) 60:1408

Tudose RC, Calotă RN, Rusu MC. Origin-entry geometry and left-sided V1 vertebral artery tortuosity: a retrospective cross-sectional CT angiography study. Neuroradiology. 2026 Sep 3. Epub ahead of print. PMID: 42690340. https://doi.org/10.1007/s00234-026-04180-9

Valdueza JM, Von Munster T, Hoffman O, Schreiber S, Einhaupl KM (2000) Postural dependency of the cerebral venous outflow. Lancet 355:200–201

Yamada H, Mizutani K, Akiyama T, Toda M (2022) Extracranial prevertebral venous network of the craniocervical junction: CT-digital subtraction venography analysis. Neuroradiology 64:2227–2233

Zhang W, Ye Y, Chen J, Wang Y, Chen R, Xiong K et al (2010a) Study on inferior petrosal sinus and its confluence pattern with relevant veins by MSCT. Surg Radiol Anat 32:563–572

Zhang WG, Ye YY, Chen JH, Chen R, Kuang LQ, Li X (2010b) Imaging study of the long extracranial extension of the inferior petrosal sinus with MSCT. Clin Anat 23:160–167

Publisher's Note Springer Nature remains neutral with regard to jurisdictional claims in published maps and institutional affiliations.